# Maximally stationary window design for overlap-add based random vibration synthesis

Damián González[a,b,*], Roberto López-Valcarce[b]

[a]*CTAG, Pol. Ind. A Granxa, 249-250, 36400 Porriño, Spain*
[b]*University of Vigo, Dept. of Signal Theory and Communications, 36310 Vigo, Spain*

**Abstract**

The accurate synthesis of realistic waveforms conforming to certain specifications is a fundamental step in random vibration testing. Since real-time implementation of digital signal processing systems for random vibration and noise synthesis necessarily operates frame by frame, the overlap-add (OLA) method, by which frames are windowed and overlapped, is widely used in practice to avoid artifacts at frame boundaries. When a wide-sense stationary random signal is desired, however, the OLA method presents a shortcoming, because the inherent periodicity of the frame-by-frame process unavoidably produces a *cyclostationary* signal, i.e., its statistics present an undesired periodic behavior. We analyze the impact of the window coefficients in the cyclostationarity properties of the synthetic process, and then present algorithms for window design with the goal of maximizing a measure of its stationarity, considering both second- and fourth-order statistical properties. The proposed designs are shown to significantly improve the stationarity properties when compared to commonly used windows.

*Keywords:* overlap-add method, synthesis window, random vibration synthesis, kurtosis, stationarity

---

[*]Corresponding author
   *Email addresses:* `damian.gonzalez@ctag.com` (Damián González),
`valcarce@gts.uvigo.es` (Roberto López-Valcarce)

## 1. Introduction

*Windowing* is a common operation which can be found in a wide range of signal processing applications. In spectral analysis, for example, desirable properties for a window include having a Fourier transform with a narrow mainlobe and low sidelobe levels with steep fall-off [1]. Another example is found in Short-Time Fourier Transform (STFT) processing of vibration and audio signals. The observed signal is split into overlapping segments, which are subsequently multiplied by an analysis window function. After STFT, frequency-domain processing (e.g., filtering by pointwise multiplication with the Discrete Fourier Transform (DFT) of the filter response), and inverse STFT to go back to the time domain, the overlap-add (OLA) method [2] can be used to reconstruct the output signal from the processed segments, which are previously multiplied by a synthesis window function. In this setting, it is common to impose on the window the constraint that, when the segments are unprocessed, the output signal be a perfect replica of the input signal, up to a processing delay. This requirement leads to the so-called *constant overlap-add* (COLA) property. The design of COLA windows with good spectral properties has been considered in [3].

Windowing is also employed in the context of random *synthesis,* which is of great interest in the fields of vibration control and testing. Random vibration controllers generate waveforms which are realizations of stochastic processes with prespecified statistical properties according to the type of vibratory environment that the device under test would experience in a real-world setting. Typical sets of specifications include (i) wide-sense stationarity (WSS), at least on a short-term basis; (ii) a predefined power spectral density (PSD) or, equivalently, a given autocorrelation function; and (iii) a given probability density function (pdf). The possibility of modifying the PSD and/or pdf during the synthesis process in real-time vibration control applications, and the need for generating very long duration signals, makes the usage of block processing a common choice [4, 5, 6]. The different signal blocks are independently synthesized according to the aforementioned specific requirements, and then concate-

nated using the OLA method with windowing in order to avoid discontinuities at the block boundaries. This approach, however, results in a synthetic process that need not preserve the statistical properties of the individual blocks, because in general these will be altered by the windowing and overlap-add operations.

<sup>35</sup> Therefore, it is of importance to understand the impact of the OLA method in the statistics of the synthetic process, as well as to properly design the window function to mitigate such impact. We note that desirable window features arising in different contexts, such as the aforementioned COLA property, need not be relevant in this framework.

<sup>40</sup> To the best of the authors' knowledge, the only references dealing with this issue are [4, 7], which endorse the use of windows resulting in a synthetic process whose variance remains constant with time; this property is achieved if the overlapped windows yield a constant sum of squares. However, this constant-variance property alone is not sufficient for the process to be truly (wide sense)

<sup>45</sup> stationary: for example, if the individual blocks have constant variance, then so does the process obtained with a rectangular window and no overlapping, yet this "direct concatenation" method is clearly undesirable for the reasons discussed above. Additionally, most commonly used windows will fulfill the constant-variance property only for specific overlap factors.

<sup>50</sup> In certain applications it is desired to synthesize non-Gaussian vibration waveforms, to more accurately reflect the vibratory environment [6, 8, 9, 10]. The degree of non-Gaussianity is typically manipulated by controlling the kurtosis of the distribution used to synthesize the individual blocks. In such cases, stationarity of the higher-order statistics should also be considered when de-

<sup>55</sup> signing the synthesis window to be used in the OLA process, since wide-sense stationarity is, by definition, only a second-order property. Kurtosis variations in the synthetic waveform may lead to an undesired increase of its crest factor, ultimately impacting structural life when durability testing is considered [11].

Motivated by the above considerations, in this paper we focus on the im-

<sup>60</sup> pact of the window function on the stationarity properties of a random process synthesized by means of the OLA method. First, it is shown that such process

3

is *cyclostationary* in general, and not WSS. Then, a cost function promoting second-order stationarity is defined and an algorithm for the computation of the corresponding optimal window is described. For the case of non-Gaussian random vibration synthesis, an analogous strategy is applied to the analysis of the stationarity of fourth-order statistics (kurtosis), and a cost function aimed at maximizing fourth-order stationarity is defined and optimized. The stationarity of the process for the proposed windows is then evaluated and compared with that obtained with other commonly used windows. Finally, conclusions are presented based on the obtained results.

The notation adopted throughout the paper is as follows. $\mathbb{E}\left\{\cdot\right\}$ denotes statistical expectation. Bold lowercase and uppercase letters represent vectors and matrices, respectively. Vectors are column vectors unless otherwise specified, the identity matrix is denoted by $\boldsymbol{I}$, and the vectors of all zeros and all ones are respectively denoted by $\boldsymbol{0}$ and $\boldsymbol{1}$. For a matrix $\boldsymbol{A}$, its transpose, conjugate, and conjugate transpose are respectively denoted by $\boldsymbol{A}^T$, $\boldsymbol{A}^*$ and $\boldsymbol{A}^H$. The 2-norm of a vector $\boldsymbol{v}$ is $\|\boldsymbol{v}\| = \sqrt{\boldsymbol{v}^T \boldsymbol{v}}$. The gradient of a function $F$ with respect to variable $\boldsymbol{w}$ is denoted by $\nabla_{\boldsymbol{w}} F(\boldsymbol{w})$. For a complex number $c$, its real and imaginary parts are respectively denoted by $\mathrm{Re}\left\{c\right\}$ and $\mathrm{Im}\left\{c\right\}$.

## 2. Second-order analysis of the overlap-add method

Consider an OLA-based synthesis system. Blocks have a length of $N$ samples, and are denoted as $x_\ell[n]$, with $\ell$ and $n$ the block and sample indices, respectively; thus, $x_\ell[n]$ is nonzero only for $n = 0$, 1,..., $N - 1$. Analogously, the length-$N$ window function $w[n]$ is defined in the interval $0 \leq n \leq N - 1$. The synthesized signal $z[n]$ is then given by

$$z[n] = \sum_{\ell=-\infty}^{\infty} w[n - \ell D] x_\ell[n - \ell D], \tag{1}$$

where $D \leq N$ is the overlap factor, or hop size. Thus, if $D < N$, there will be overlapping between consecutive blocks.

In practice, a set of requirements are imposed on the statistics of $z[n]$, whereas one has freedom to establish those of the individual blocks. Thus, we investigate the statistical properties of $z[n]$, given those of $x_\ell[n]$ and the OLA synthesis equation (1). To proceed with the analysis, the following assumptions on the random blocks $x_\ell[n]$, $n = 0, 1, \ldots, N - 1$, will be adopted throughout.

A1. The mean is zero: $\mathbb{E}\{x_\ell[n]\} = 0$ for all $\ell$, $n$.

A2. Different blocks are uncorrelated: $\mathbb{E}\{x_\ell[n]x_m[s]\} = \mathbb{E}\{x_\ell[n]\}\mathbb{E}\{x_m[s]\}$ for $\ell \neq m$.

A3. Blocks are WSS with the same autocorrelation: $\mathbb{E}\{x_\ell[n]x_\ell[s]\}$ depends only on the time difference $n - s$, and not on $\ell$.

Assumption A1 is reasonable given the nature of commonly found vibration signals, whose mean acceleration is zero. Assumption A2 depends on the particular synthesis algorithm, but can be easily achieved if blocks are generated independently, as it is usually the case in practice [4]. Assumption A3 requires that the baseline block process be WSS stationary itself, and is reasonable whenever the final goal is to synthesize a WSS signal $z[n]$.

Given a window $w[n]$, consider the statistics of the synthesized process $z[n]$ in (1). By Assumption A1, its first-order moment (i.e., its mean) is

$$\mathbb{E}\{z[n]\} = \sum_\ell w[n - \ell D]\,\mathbb{E}\{x_\ell[n - \ell D]\} = 0. \tag{2}$$

Thus, the OLA process preserves the zero-mean property.

Consider now the second-order statistics of $z[n]$. By virtue of Assumption A3, we will denote the autocorrelation function of the blocks by

$$r_x[\tau] \triangleq \mathbb{E}\{x_\ell[n]x_\ell[n - \tau]\}. \tag{3}$$

5

100    Then the autocorrelation of $z[n]$ can be expressed in terms of $r_x[\tau]$ as

$$
\begin{aligned}
r_z[n;\tau] &\triangleq \mathbb{E}\left\{z[n]z[n-\tau]\right\} \\
&= \sum_\ell \sum_m w[n-\ell D]w[n-\tau-mD]\,\mathbb{E}\left\{x_\ell[n-\ell D]x_m[n-\tau-mD]\right\} \\
&= \sum_\ell w[n-\ell D]w[n-\tau-\ell D]\,\mathbb{E}\left\{x_\ell[n-\ell D]x_\ell[n-\tau-\ell D]\right\} \qquad (4) \\
&= r_x[\tau]\sum_\ell w[n-\ell D]w[n-\tau-\ell D], \qquad\qquad\qquad\qquad\qquad (5)
\end{aligned}
$$

where in (4) we have used Assumption A2, and in (5) we used Assumption A3.

Denoting now[1]

$$
r_w[n;\tau] \triangleq \sum_{\ell=-\infty}^{\infty} w[n-\ell D]w[n-\tau-\ell D], \qquad (6)
$$

one has from (5) that

$$
r_z[n;\tau] = r_x[\tau]r_w[n;\tau]. \qquad (7)
$$

The process $z[n]$ is WSS iff $r_z[n;\tau]$ does not depend on $n$. In general, $r_w[n;\tau]$ will not be constant with $n$, and hence $z[n]$ will not be WSS. However, $z[n]$ is *cyclostationary* [12] with period $D$, i.e., its autocorrelation is $D$-periodic in $n$:

$$
r_z[n+D;\tau] = r_z[n;\tau] \qquad \text{for all } n, \qquad (8)
$$

which follows immediately from the fact that $r_w[n;\tau]$ in (6) is periodic in $n$ with period $D$. This periodicity allows one to write $r_w[n;\tau]$ as a Fourier series [13]:

$$
r_w[n;\tau] = \sum_{k=0}^{D-1} c_w[k;\tau]e^{j\frac{2\pi}{D}kn}, \qquad (9)
$$

where $c_w[k;\tau]$, $0 \leq k \leq D-1$, are the Fourier coefficients (also known as *cyclic correlations*), given by

$$
c_w[k;\tau] = \frac{1}{D}\sum_{n=0}^{D-1} r_w[n;\tau]e^{-j\frac{2\pi}{D}kn}. \qquad (10)
$$

---

[1]Note that $r_w[n;\tau]$ depends on the hop size $D$. For simplicity, we do not make this dependence explicit in the notation.

In view of (9), $r_w[n; \tau]$ is constant with $n$ iff $c_w[k; \tau] = 0$ for $k = 1, \ldots, D - 1$.

Using (6), these Fourier coefficients can be written as

$$
\begin{aligned}
c_w[k; \tau] &= \frac{1}{D} \sum_{n=0}^{D-1} \sum_{\ell=-\infty}^{\infty} w[n - \ell D] w[n - \tau - \ell D] e^{-j\frac{2\pi}{D}kn} \\
&= \frac{1}{D} \sum_{m=-\infty}^{\infty} w[m] w[m - \tau] e^{-j\frac{2\pi}{D}km} \quad\quad (11) \\
&= \frac{1}{D} \left( w[\tau] e^{-j\frac{2\pi}{D}k\tau} \right) \star w[-\tau], \quad\quad (12)
\end{aligned}
$$

with $\star$ denoting convolution. Thus, $c_w[k; \tau]$ is seen to be the crosscorrelation between the window function and a spectrally shifted replica of itself. For $k = 0$, $c_w[0; \tau]$ reduces (up to a scaling) to the standard autocorrelation $w[\tau] \star w[-\tau]$.

## 3. Window design for second-order stationarity

Assuming that the final goal is to generate a WSS process $z[n]$, the previous analysis shows that the OLA method poses a problem in this regard, as the cyclostationary character of $z[n]$ is an artifact due to the synthesis process and not a desirable feature. It is reasonable then to ask if it is possible to pick the window function in order to have a process $z[n]$ "as stationary as possible". To this end, first we introduce a measure of wide-sense stationarity, and then we will consider the optimization of the window according to this metric.

### 3.1. A cost function promoting wide-sense stationarity

Particularizing (7) for $\tau = 0$, the expression for the time fluctuations of the variance of the process $z[n]$, given by $\mathbb{E}\left\{ z^2[n] \right\} = r_z[n; 0]$, is obtained:

$$
r_z[n; 0] = r_x[0] r_w[n; 0] = r_x[0] \sum_{\ell=-\infty}^{\infty} w^2[n - \ell D]. \quad\quad (13)
$$

Therefore, in order to have constant variance with time, the window must satisfy

$$
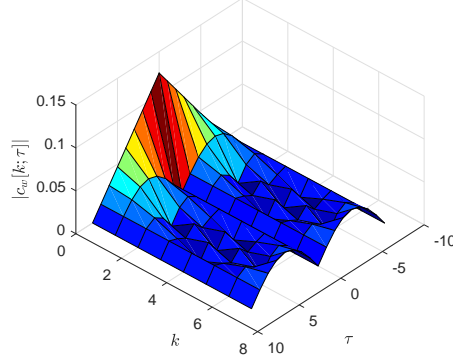\sum_{\ell=-\infty}^{\infty} w^2[n - \ell D] = \text{constant.} \quad\quad (14)
$$

7

Figure 1: Magnitude of the Fourier coefficients $c_w[k;\tau]$ for a rectangular window of length $N = 8$ and no overlap ($D = N$), indicating significant non-stationarity.

This was recognized in [7], where the authors proposed the use of a half-sinusoid window $w[n] = \sin\frac{\pi(n+\frac{1}{2})}{N}$, $0 \leq n \leq N - 1$, which satisfies (14) for $D = N/2$. In [4], the constant variance property (14) is used as the stationarity criterion for evaluating synthesis window performance. In terms of the cyclic correlations $c_w[k;\tau]$, (14) is equivalent to having $c_w[k;0] = 0$ for $k = 1, \ldots, D-1$.

However, constant variance is *not* equivalent to wide-sense stationarity. For example, for any hop size $D$ such that $N/D$ is an integer, the rectangular (or boxcar) window $w[n] = 1$, $0 \leq n \leq N - 1$, satisfies (14); however, the degree of nonstationarity in that case is rather high, as evidenced by the fluctuations with $n$ of the remaining correlation coefficients $r_z[n;\tau]$ with $\tau \neq 0$; equivalently, the cyclic correlations $c_w[k;\tau]$, $k = 1, \ldots, D - 1$ may take nonzero values for $\tau \neq 0$. To illustrate this, Fig. 1 shows the magnitude of the Fourier coefficients $c_w[k;\tau]$ for a rectangular window of length $N = 8$ and no overlap ($D = N$). Significant magnitude values are clearly seen for $k > 0$, indicating lack of stationarity.

The above considerations indicate that the process $z[n]$ will be closer to being WSS if the cyclic correlations $c_w[k;\tau]$ had small magnitudes for all $\tau$ and $k = 1, \ldots, D - 1$. This observation suggests one possible approach to window design. Letting $\boldsymbol{w} \triangleq \begin{bmatrix} w[0] & w[1] & \cdots & w[N-1] \end{bmatrix}^T \in \mathbb{R}^N$ be the vector of

8

window coefficients, consider the cost function

$$J_2(\boldsymbol{w}) \triangleq \sum_{k=1}^{D-1} \sum_{|\tau|<N} |c_w[k;\tau]|^2 . \tag{15}$$

We propose to pick $\boldsymbol{w}$ in order to minimize $J_2(\boldsymbol{w})$. To avoid the trivial solution $\boldsymbol{w} = \boldsymbol{0}$, a suitable constraint has to be placed, e.g., $\|\boldsymbol{w}\|^2 = 1$, or equivalently $c_w[0;0] = \frac{1}{D}$. Note from (6) that $r_w[n;\tau] = 0$ for $|\tau| \geq N$ since the window has length $N$; in view of (10), $c_w[k;\tau] = 0$ for $|\tau| \geq N$ as well. Therefore, it suffices to consider the range $|\tau| < N$ in the inner summation in (15).

In order to expose the dependence of $J_2$ with the parameter $\boldsymbol{w}$, let us introduce the $N \times N$ matrices $\boldsymbol{S}, \boldsymbol{\Gamma}$ as

$$[\boldsymbol{S}]_{i,j} = \begin{cases} 1, & j-i=1, \\ 0, & \text{else}, \end{cases} \tag{16}$$

$$\boldsymbol{\Gamma} = \text{diag}\left\{ \begin{array}{ccccc} 1 & e^{-j\frac{2\pi}{D}} & e^{-j\frac{2\pi}{D}2} & \cdots & e^{-j\frac{2\pi}{D}(N-1)} \end{array} \right\}. \tag{17}$$

Note that $\boldsymbol{S}$ is an upper shift matrix, i.e., $\boldsymbol{Sw}$ is a vector obtained by shifting the entries of $\boldsymbol{w}$ one position in the upward direction. We shall use the convention $\boldsymbol{S}^0 = \boldsymbol{I}$ and $\boldsymbol{S}^\tau = (\boldsymbol{S}^{|\tau|})^T$ for $\tau < 0$. (Note that $\boldsymbol{S}^T$ is a *lower* shift matrix). Then, the cyclic correlations can be written for all $k$ and $\tau$ as

$$c_w[k;\tau] = \frac{1}{D}\boldsymbol{w}^T \boldsymbol{A}_{\tau k}\boldsymbol{w}, \qquad \text{with} \qquad \boldsymbol{A}_{\tau k} \triangleq \boldsymbol{S}^\tau \boldsymbol{\Gamma}^k. \tag{18}$$

Using (18), the cost (15) can be expressed as

$$J_2(\boldsymbol{w}) = \frac{1}{D^2} \sum_{k=1}^{D-1} \sum_{|\tau|<N} \left| \boldsymbol{w}^T \boldsymbol{A}_{\tau k}\boldsymbol{w} \right|^2 . \tag{19}$$

*3.2. Minimization of $J_2$*

The function $J_2$ in (19) is nonquadratic in $\boldsymbol{w}$, so it seems difficult to obtain the minimizer (under the constraint $\|\boldsymbol{w}\|^2 = 1$) in closed form. Nevertheless, it is possible to obtain first-order conditions on the solutions of this problem, which will be useful in order to derive efficient numerical schemes.

Consider the Lagrangian for the minimization of $J_2(\boldsymbol{w})$ subject to $\boldsymbol{w}^T\boldsymbol{w} = 1$:

$$L(\boldsymbol{w}) = J_2(\boldsymbol{w}) + \lambda(1 - \boldsymbol{w}^T\boldsymbol{w}), \tag{20}$$

9

where $\lambda$ is the Lagrange multiplier. Then, any (local) minimum $\boldsymbol{w}_\star$ of this problem must satisfy the first-order condition $\nabla_{\boldsymbol{w}} L(\boldsymbol{w}_\star) = \nabla_{\boldsymbol{w}} J_2(\boldsymbol{w}_\star) - 2\lambda \boldsymbol{w}_\star = \boldsymbol{0}$. These are only necessary conditions, as they may be satisfied by other points which are not local minima (e.g., maxima or saddle points). The expression of $\nabla_{\boldsymbol{w}} J_2(\boldsymbol{w})$ is given in the following result, whose proof is in the Appendix.

**Lemma 1.** *Define the $N \times N$ Hermitian positive (semi)definite matrices*

$$\boldsymbol{A}(\boldsymbol{w}) \triangleq \frac{1}{D^2} \sum_{k=1}^{D-1} \sum_{|\tau| < N} \boldsymbol{A}_{\tau k} \boldsymbol{w} \boldsymbol{w}^T \boldsymbol{A}_{\tau k}^H, \tag{21}$$

$$\boldsymbol{B}(\boldsymbol{w}) \triangleq \frac{1}{D^2} \sum_{k=1}^{D-1} \sum_{|\tau| < N} \boldsymbol{A}_{\tau k}^T \boldsymbol{w} \boldsymbol{w}^T \boldsymbol{A}_{\tau k}^*. \tag{22}$$

*Then the gradient $\nabla_{\boldsymbol{w}} J_2(\boldsymbol{w})$ satisfies*

$$\nabla_{\boldsymbol{w}} J_2(\boldsymbol{w}) = 2 \operatorname{Re} \{ \boldsymbol{A}(\boldsymbol{w}) + \boldsymbol{B}(\boldsymbol{w}) \} \boldsymbol{w}. \tag{23}$$

The computation of $\boldsymbol{A}(\boldsymbol{w})$, $\boldsymbol{B}(\boldsymbol{w})$ featuring in (23) can be significantly simplified, as the following result states; see the Appendix for the proof.

**Lemma 2.** *$\boldsymbol{A}(\boldsymbol{w})$ is real-valued and Toeplitz, and its first column is given by*

$$[\boldsymbol{A}(\boldsymbol{w})]_{i,0} = \frac{\alpha[i]}{D^2} \sum_{\ell=0}^{N-1-i} w[i+\ell]w[\ell] \qquad i = 0, 1, \ldots, N-1, \tag{24}$$

*where the sequence $\alpha[i]$ is defined as*

$$\alpha[i] \triangleq \begin{cases} D-1, & i = 0, \pm D, \pm 2D, \ldots, \\ -1, & \text{otherwise.} \end{cases} \tag{25}$$

*Moreover, it holds that $\boldsymbol{B}(\boldsymbol{w}) = \boldsymbol{A}(\boldsymbol{w})$.*

Therefore, from Lemmas 1 and 2, the gradient of the Lagrangian is

$$\nabla_{\boldsymbol{w}} L(\boldsymbol{w}) = \nabla_{\boldsymbol{w}} J_2(\boldsymbol{w}) - 2\lambda \boldsymbol{w} = 4\boldsymbol{A}(\boldsymbol{w})\boldsymbol{w} - 2\lambda \boldsymbol{w}, \tag{26}$$

so that the first-order condition $\nabla_{\boldsymbol{w}} L(\boldsymbol{w}_\star) = \boldsymbol{0}$ reads as

$$\boldsymbol{A}(\boldsymbol{w}_\star)\boldsymbol{w}_\star = \frac{\lambda}{2} \boldsymbol{w}_\star, \tag{27}$$

i.e., $\boldsymbol{w}_\star$ is a unit-norm eigenvector of $\boldsymbol{A}(\boldsymbol{w}_\star)$, with associated eigenvalue $\lambda/2$.

Given the definition of $\boldsymbol{A}(\boldsymbol{w})$ in (21), it is readily checked that, for any $\boldsymbol{w} \in \mathbb{R}^N$, the cost $J_2(\boldsymbol{w})$ in (19) can be written as

$$J_2(\boldsymbol{w}) = \boldsymbol{w}^T \boldsymbol{A}(\boldsymbol{w})\boldsymbol{w}. \tag{28}$$

In view of (27) and (28), it is seen that if $\boldsymbol{w}_\star$ satisfies the first-order condition, then the cost at such point equals $J_2(\boldsymbol{w}_\star) = \frac{\lambda}{2}$, which is an eigenvalue of $\boldsymbol{A}(\boldsymbol{w}_\star)$.

### 3.3. Iterative algorithms

The first-order condition tells us that the vector $\boldsymbol{w}_\star$ minimizing $J_2$ is an eigenvector of $\boldsymbol{A}(\boldsymbol{w}_\star)$ with associated eigenvalue $J_2(\boldsymbol{w}_\star)$; however, it does not reveal *which* eigenvalue it must be. Since our goal is to minimize $J_2$, one may hope that the corresponding eigenvalue be the *smallest.* If that was the case, it would make sense to construct a sequence of estimates as follows. Starting with some initial candidate window $\boldsymbol{w}_0$ with $\|\boldsymbol{w}_0\| = 1$ (for example, the normalized rectangular window: $\boldsymbol{w}_0 = \frac{1}{\sqrt{N}}\boldsymbol{1}$), then for $k = 1, 2, \ldots$, compute:

$$\boldsymbol{w}_k = \text{least unit-norm eigenvector of } \boldsymbol{A}(\boldsymbol{w}_{k-1}). \tag{29}$$

In this way, if the sequence $\{\boldsymbol{w}_k\}$ obtained by repeated application of (29) converges to some $\boldsymbol{w}_\star$, then such $\boldsymbol{w}_\star$ satisfies the first-order condition, and $J_2(\boldsymbol{w}_\star)$ is the smallest eigenvalue of $\boldsymbol{A}(\boldsymbol{w}_\star)$.

Iteration (29) requires an eigenvector extraction at each step. This can be achieved by using the *inverse power method* [14], in which the least eigenvector of a symmetric positive definite matrix $\boldsymbol{M}$ is successively approximated by solving $\boldsymbol{M}\boldsymbol{y}_n = \boldsymbol{x}_{n-1}$ and setting $\boldsymbol{x}_n = \boldsymbol{y}_n/\|\boldsymbol{y}_n\|$. In this way, we would have an *inner* iteration (running the inverse power method for a prespecified number of steps) embedded within an *outer* iteration given by (29). If only a single inner iteration is performed, the scheme boils down to:

$$\text{For } k = 1, 2, \ldots, \text{ solve} \quad \boldsymbol{A}(\boldsymbol{w}_{k-1})\boldsymbol{v}_k = \boldsymbol{w}_{k-1} \quad \text{and set} \quad \boldsymbol{w}_k = \frac{\boldsymbol{v}_k}{\|\boldsymbol{v}_k\|}. \tag{30}$$

If the sequence $\{\boldsymbol{w}_k\}$ in (30) converges to some point $\boldsymbol{w}_\star$, then again $\boldsymbol{w}_\star$ satisfies the first-order condition. However, it is not clear whether in this case $J_2(\boldsymbol{w}_\star)$

11

is the smallest eigenvalue of $\boldsymbol{A}(\boldsymbol{w}_\star)$. Simulation results suggest that, when initialized with the same value, both iterations (29) and (30) converge to the same setting, although iteration (30) has the advantage of computational simplicity.

### 4. Window design for fourth-order stationarity

In many occasions, it is desired that the synthesized process be non-Gaussian. A common approach is to assume zero skewness (ratio of third moment to standard deviation cubed) and specify its kurtosis (ratio of fourth moment to the variance squared; for a Gaussian distribution, the kurtosis equals 3) [15, 16, 17]. Hence, it is of interest to analyze the impact of the OLA method on higher-order statistics, in a similar vein of the second-order analysis presented in previous sections. To this end, we will adopt an additional assumption on the fourth-order statistics of the random blocks $x_\ell[n]$:

A4. Blocks are fourth-order stationary, so that their *quadri-autocorrelation function,* defined as

$$\mathfrak{r}_x[\boldsymbol{\tau}] \triangleq \mathbb{E}\left\{x_\ell[n]x_\ell[n-\tau_1]x_\ell[n-\tau_2]x_\ell[n-\tau_3]\right\}, \tag{31}$$

depends only on $\boldsymbol{\tau} \triangleq [\ \tau_1 \quad \tau_2 \quad \tau_3\ ]$, but not on $n$ or $\ell$.

In order to analyze the fourth-order statistics of the synthesized process $z[n]$, let us define its quadri-autocorrelation function as

$$\mathfrak{r}_z[n;\boldsymbol{\tau}] \triangleq \mathbb{E}\left\{z[n]z[n-\tau_1]z[n-\tau_2]z[n-\tau_3]\right\} \tag{32}$$

$$= \sum_{\ell_0\cdots\ell_3} w[n-\ell_0 D]w[n-\ell_1 D-\tau_1]w[n-\ell_2 D-\tau_2]w[n-\ell_3 D-\tau_3] \times$$
$$\mathbb{E}\left\{x_{\ell_0}[n-\ell_0 D]x_{\ell_1}[n-\ell_1 D-\tau_1]x_{\ell_2}[n-\ell_2 D-\tau_2]x_{\ell_3}[n-\ell_3 D-\tau_3]\right\} \tag{33}$$

Using assumptions A2, A3 and A4, <span style="color:red">it</span> is found that (33) can be written as

$$\begin{aligned}
\mathfrak{r}_z[n;\boldsymbol{\tau}] &= \mathfrak{r}_x[\boldsymbol{\tau}] \cdot \mathfrak{r}_w[n;\boldsymbol{\tau}] \\
&\quad + r_x[\tau_1] \cdot r_x[\tau_3 - \tau_2] \cdot \left(r_w[n;\tau_1] \cdot r_w[n-\tau_2;\tau_3-\tau_2] - \mathfrak{r}_w[n;\boldsymbol{\tau}]\right) \\
&\quad + r_x[\tau_2] \cdot r_x[\tau_3 - \tau_1] \cdot \left(r_w[n;\tau_2] \cdot r_w[n-\tau_3;\tau_1-\tau_3] - \mathfrak{r}_w[n;\boldsymbol{\tau}]\right) \\
&\quad + r_x[\tau_3] \cdot r_x[\tau_2 - \tau_1] \cdot \left(r_w[n;\tau_3] \cdot r_w[n-\tau_1;\tau_2-\tau_1] - \mathfrak{r}_w[n;\boldsymbol{\tau}]\right) \tag{34}
\end{aligned}$$

12

where $r_w[n; \tau]$ was defined in (6), and we have introduced the function

$$\mathfrak{r}_w[n; \boldsymbol{\tau}] \triangleq \sum_\ell w[n - \ell D]w[n - \ell D - \tau_1]w[n - \ell D - \tau_2]w[n - \ell D - \tau_3]. \quad (35)$$

Note that $\mathfrak{r}_w[n; \boldsymbol{\tau}]$ is $D$-periodic in $n$, analogously to $r_w[n; \tau]$. It follows that the quadri-autocorrelation (34) is also $D$-periodic in $n$, so that the process $z[n]$ is fourth-order cyclostationary.

The fourth moment of $z[n]$ is obtained by taking $\boldsymbol{\tau} = \mathbf{0}$ in (34):

$$\mathbb{E}\left\{z^4[n]\right\} = \mathfrak{r}_z[n; \mathbf{0}] = (\mathfrak{r}_x[\mathbf{0}] - 3r_x^2[0])\mathfrak{r}_w[n; \mathbf{0}] + 3r_x^2[0]r_w^2[n; 0], \quad (36)$$

whereas in view of (13), the second moment (variance) is $\mathbb{E}\left\{z^2[n]\right\} = r_x[0]r_w[n; 0]$. Therefore, the kurtosis of $z[n]$ can be written as

$$
\begin{aligned}
\beta_z[n] &\triangleq \frac{\mathbb{E}\{z^4[n]\}}{\mathbb{E}^2\{z^2[n]\}} = \frac{\mathfrak{r}_z[n; \mathbf{0}]}{r_z^2[n; 0]} \\
&= \beta_x \rho_w[n] + 3(1 - \rho_w[n]),
\end{aligned} \quad (37)
$$

where $\beta_x$ is the kurtosis of the individual blocks:

$$\beta_x \triangleq \frac{\mathfrak{r}_x[\mathbf{0}]}{r_x^2[0]} = \frac{\mathbb{E}\left\{x_\ell^4[n]\right\}}{\mathbb{E}^2\{x_\ell^2[n]\}}, \quad (38)$$

and the $D$-periodic function $\rho_w[n]$ is defined as

$$\rho_w[n] \triangleq \frac{\mathfrak{r}_w[n; \mathbf{0}]}{r_w^2[n; 0]} = \frac{\sum_\ell w^4[n - \ell D]}{\left(\sum_\ell w^2[n - \ell D]\right)^2}. \quad (39)$$

Note that $0 \leq \rho_w[n] \leq 1$, since

$$
\begin{aligned}
\left(\sum_\ell w^2[n - \ell D]\right)^2 &= \sum_\ell \sum_m w^2[n - \ell D]w^2[n - mD] \\
&= \sum_\ell w^4[n - \ell D] + \sum_\ell \sum_{m \neq \ell} w^2[n - \ell D]w^2[n - mD] \\
&\geq \sum_\ell w^4[n - \ell D] \qquad \text{for all } n. \quad (40)
\end{aligned}
$$

Hence, (37) shows that the kurtosis $\beta_z[n]$ is a (time-varying, and in fact, $D$-periodic) convex combination of the kurtosis $\beta_x$ and that of a Gaussian random variable, which is 3. This means that the OLA synthesis method yields a ($D$-periodic) kurtosis which is closer to that of a Gaussian, or in other words,

13

after OLA, the resulting process is "closer to Gaussian". This makes sense, because the OLA method constructs $z[n]$ as the sum of a number of statistically independent random variables, see (1); the larger the number of terms in the sum, the closer the distribution will be to a Gaussian, asymptotically reaching this distribution by virtue of the Central Limit Theorem. When the individual blocks are Gaussian ($\beta_x = 3$), then (37) shows that $\beta_z[n] = 3$ for all $n$, so that the synthetisized process is Gaussian as well, as it should be since in such case $z[n]$ is a linear combination of Gaussian random variables. For non-Gaussian synthesis $\beta_x \neq 3$, and the kurtosis $\beta_z[n]$ will be constant with $n$ iff $\rho_w[n]$ is constant. Therefore, in practice we would like $\rho_w[n]$ to be as constant and as close to 1 as possible. For example, for a rectangular window and hop factor $D$ such that $N/D$ is an integer, $\rho_w[n]$ is constant and equal to $\frac{D}{N} \leq 1$.

However, similarly to the situation in Sec. 3 regarding the temporal fluctuations of the variance, having a constant kurtosis does not necessarily translate into (fourth-order) stationarity. Again, for hop size $D = N$ (no overlap) a rectangular window would result in constant variance and constant kurtosis $\beta_z[n] = \beta_x$ (since $\rho_w[n] = 1$ for all $n$), but it would also yield a high degree of nonstationarity, as shown in Fig. 1. For this reason, we explore next the design of windows with good fourth-order stationarity properties, in the sense that we would like the quadri-autocorrelation function $\mathfrak{r}_z[n; \boldsymbol{\tau}]$ in (34) to be independent of $n$. For this, both $r_w[n; \tau]$ and $\mathfrak{r}_w[n; \boldsymbol{\tau}]$ should be constant with $n$. A similar approach to the *second-order* case can be applied to *fourth-order* stationarity.

To this end, since $\mathfrak{r}_w[n; \boldsymbol{\tau}]$ is $D$-periodic in $n$, it can be written as

$$\mathfrak{r}_w[n; \boldsymbol{\tau}] = \sum_{k=0}^{D-1} \mathfrak{c}_w[k; \boldsymbol{\tau}] e^{j\frac{2\pi}{D}kn}, \tag{41}$$

where $\mathfrak{c}_w[k; \boldsymbol{\tau}]$ are the Fourier coefficients (*cyclic quadri-correlations*), given by

$$\mathfrak{c}_w[k; \boldsymbol{\tau}] = \frac{1}{D} \sum_{n=0}^{D-1} \mathfrak{r}_w[n; \boldsymbol{\tau}] e^{-j\frac{2\pi}{D}kn}. \tag{42}$$

14

Using (35), the cyclic quadri-correlations can be written as

$$
\begin{aligned}
\mathfrak{c}_w[k; \boldsymbol{\tau}] &= \frac{1}{D} \sum_{n=0}^{D-1} \sum_{\ell=-\infty}^{\infty} w[n - \ell D] w[n - \ell D - \tau_1] w[n - \ell D - \tau_2] w[n - \ell D - \tau_3] e^{-j\frac{2\pi}{D} kn} \\
&= \frac{1}{D} \sum_{m=-\infty}^{\infty} w[m] w[m - \tau_1] w[m - \tau_2] w[m - \tau_3] e^{-j\frac{2\pi}{D} km}.
\end{aligned} \tag{43}
$$

Our approach at this point is analogous to that from Sec. 3.1: to design a window for which $\mathfrak{r}_w[n; \boldsymbol{\tau}]$ is as constant with $n$ as possible, we propose to minimize the sum of squares of all cyclic quadri-correlations with $k \neq 0$, given by

$$
J_4(\boldsymbol{w}) \triangleq \sum_{k=1}^{D-1} \sum_{|\tau_1|<N} \sum_{|\tau_2|<N} \sum_{|\tau_3|<N} |\mathfrak{c}_w[k; \boldsymbol{\tau}]|^2. \tag{44}
$$

In order to find a suitable expression for $J_4(\boldsymbol{w})$, substitute (43) in (44) to obtain

$$
\begin{aligned}
J_4(\boldsymbol{w}) &= \frac{1}{D^2} \sum_{|\tau_1|<N} \sum_{|\tau_2|<N} \sum_{|\tau_3|<N} \sum_{p} \sum_{q} w[p] w[p - \tau_1] w[p - \tau_2] w[p - \tau_3] \\
&\quad \times w[q] w[q - \tau_1] w[q - \tau_2] w[q - \tau_3] \left( \sum_{k=1}^{D-1} e^{-j\frac{2\pi}{D} k(p-q)} \right).
\end{aligned} \tag{45}
$$

The term in parentheses in (45) is $\alpha[p-q]$, with $\alpha[n]$ defined in (25). Therefore,

$$
\begin{aligned}
J_4(\boldsymbol{w}) &= \sum_{p} \sum_{q} w[p] w[q] \left[ \frac{\alpha[p-q]}{D^2} \left( \sum_{|\tau_1|<N} w[p - \tau_1] w[q - \tau_1] \right) \right. \\
&\quad \left. \times \left( \sum_{|\tau_2|<N} w[p - \tau_2] w[q - \tau_2] \right) \left( \sum_{|\tau_3|<N} w[p - \tau_3] w[q - \tau_3] \right) \right] (46)
\end{aligned}
$$

The three terms in parentheses in (46) are all equal, and they are given by the autocorrelation of the window, i.e., $w[n] \star w[-n]$, evaluated at $n = p - q$. Therefore, if we define the $N \times N$ symmetric Toeplitz matrix $\boldsymbol{K}(\boldsymbol{w})$ with elements in its first column given by

$$
[\boldsymbol{K}(\boldsymbol{w})]_{i,0} = \frac{\alpha[i]}{D^2} \left( \sum_{\ell=0}^{N-1-i} w[i + \ell] w[\ell] \right)^3, \qquad i = 0, 1, \ldots, N-1, \tag{47}
$$

then (46) can be written as

$$
\begin{aligned}
J_4(\boldsymbol{w}) &= \sum_{p} \sum_{q} w[p] w[q] [\boldsymbol{K}(\boldsymbol{w})]_{p,q} \\
&= \boldsymbol{w}^T \boldsymbol{K}(\boldsymbol{w}) \boldsymbol{w},
\end{aligned} \tag{48}
$$

15

an expression which is similar to that corresponding to the second-order cost function $J_2(\boldsymbol{w})$, see (28). Note, however, that whereas the elements of the matrix $\boldsymbol{A}(\boldsymbol{w})$ in (28) are quadratic functions of $\boldsymbol{w}$, those of $\boldsymbol{K}(\boldsymbol{w})$ are of sixth-order.

In any case, one may apply the same procedure as in Sec. 3.3 to numerically find a minimum of $J_4(\boldsymbol{w})$, for example:

$$\text{for } k = 1, 2, \ldots, \text{ set } \quad \boldsymbol{w}_k = \text{least unit-norm eigenvector of } \boldsymbol{K}(\boldsymbol{w}_{k-1}), \quad (49)$$

or, if eigenvector extractions are to be avoided,

$$\text{for } k = 1, 2, \ldots, \text{ solve } \quad \boldsymbol{K}(\boldsymbol{w}_{k-1})\boldsymbol{v}_k = \boldsymbol{w}_{k-1} \quad \text{and set} \quad \boldsymbol{w}_k = \frac{\boldsymbol{v}_k}{\|\boldsymbol{v}_k\|}. \quad (50)$$

These iterations were found to converge in all tested cases, and no numerical problems have been observed.

## 5. Results and discussion

We focus on the results obtained by iterations (30) and (50) initialized with the rectangular window $\boldsymbol{w}_0 = \frac{1}{\sqrt{N}}\boldsymbol{1}$, as these are computationally simpler than (29) and (49), and as already mentioned, iterations (29)-(30) both converged to the same point in all tested cases, and so did iterations (49)-(50).

Figs. 2 and 3 show the results for a block length $N = 256$ and different values of the hop size $D$, considering second and fourth-order stationarity optimization, respectively. In all cases, convergence was achieved in 10 iterations or less. For small overlap percentages, the improvement with respect to the rectangular window is small; this makes sense, because with small overlap it is very difficult to counteract the artifacts introduced by block-by-block processing. However, as the amount of overlap increases, the improvement achieved by the proposed window designs becomes more pronounced. For example, for $D = N/4$ (75% overlap) and second-order stationarity, the achieved cost is almost four orders of magnitude smaller than that for the rectangular window, and the resulting design yields a function $r_w[n; \tau]$ which is practically constant with $n$.

Assuming a "second-order quasi-stationary" window such that $r_w[n; \tau] \approx r_w[\tau]$, the autocorrelation of the synthesized process $z[n]$ becomes $r_z[\tau] \approx r_x[\tau]r_w[\tau]$.
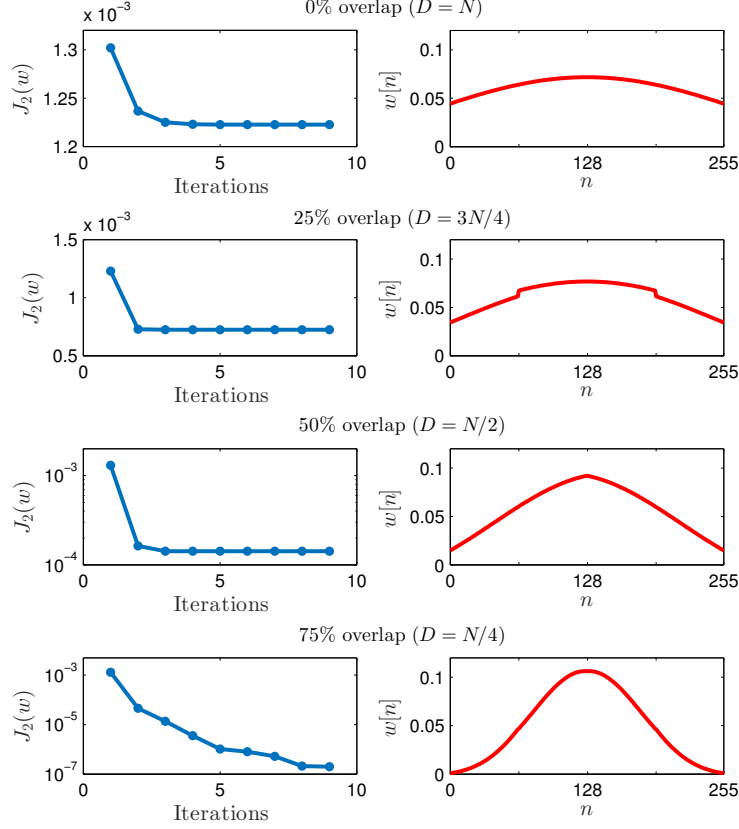
16

Figure 2: Results obtained for second-order stationarity optimization, $N = 256$ and different overlap factors. Left: convergence of the cost function $J_2$. Right: resulting window $w[n]$.

Equivalently, its power spectral density (PSD) is the convolution of that of the individual blocks and the Fourier transform of $r_w[\tau]$, which is $|W(e^{j\omega})|^2$, with

$$W(e^{j\omega}) = \sum_{n=0}^{N-1} w[n]e^{-j\frac{2\pi}{k}n} \tag{51}$$

the Fourier transform of the window $w[n]$. This means that the windowing process has the effect of smearing the original PSD, a situation analogous to that in spectral analysis [1]. Thus, in order to limit the loss in spectral resolution, windows with narrow bandwidth and low sidelobes are desirable. Fig. 4 shows the spectra of the proposed designs together with those of commonly used windows, for $N = 256$. As the overlapping factor increases, the designed windows depart
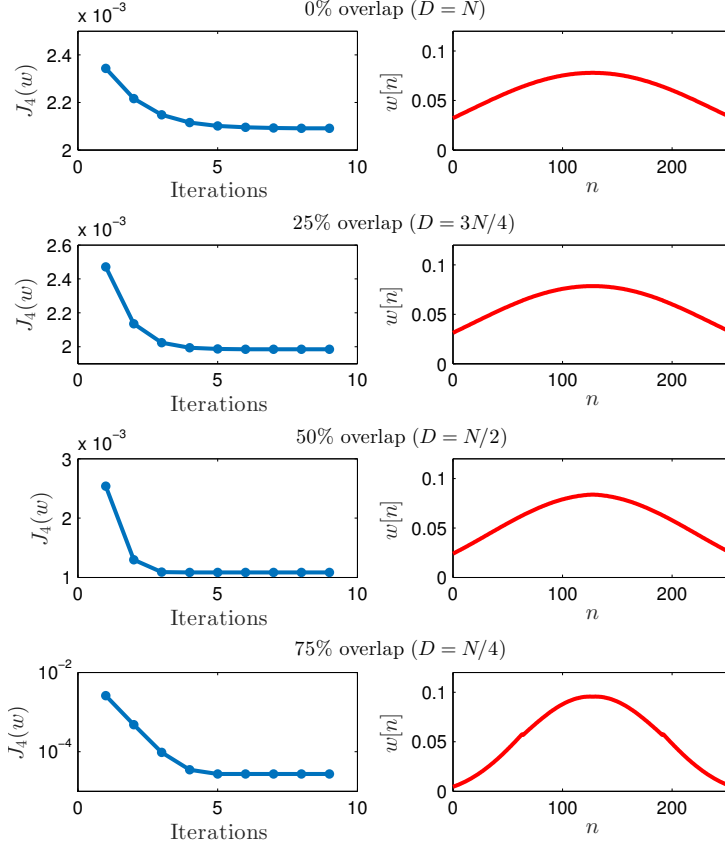
17

Figure 3: Results obtained for fourth-order stationarity optimization, $N = 256$ and different overlap factors. Left: convergence of the cost function $J_4$. Right: resulting window $w[n]$.

240  from the rectangular one: the bandwidth of the main lobe increases, whereas the sidelobe amplitudes decrease. This effect is particularly pronounced for the truly "quasi-stationary" window obtained for 75% overlap.

This effect raises an interesting issue: the frames $x_\ell[n]$ should be generated with an autocorrelation $r_x[\tau]$ that is somehow pre-compensated in order to 245  account for the fact that $r_z[\tau] \approx r_x[\tau]r_w[\tau]$, so that the synthesized process $z[n]$ has the desired autocorrelation (and therefore PSD). Within the context of closed-loop vibration control, the adjustment of the process PSD can be left to the iterative control loop, although, since the window coefficients are known, it
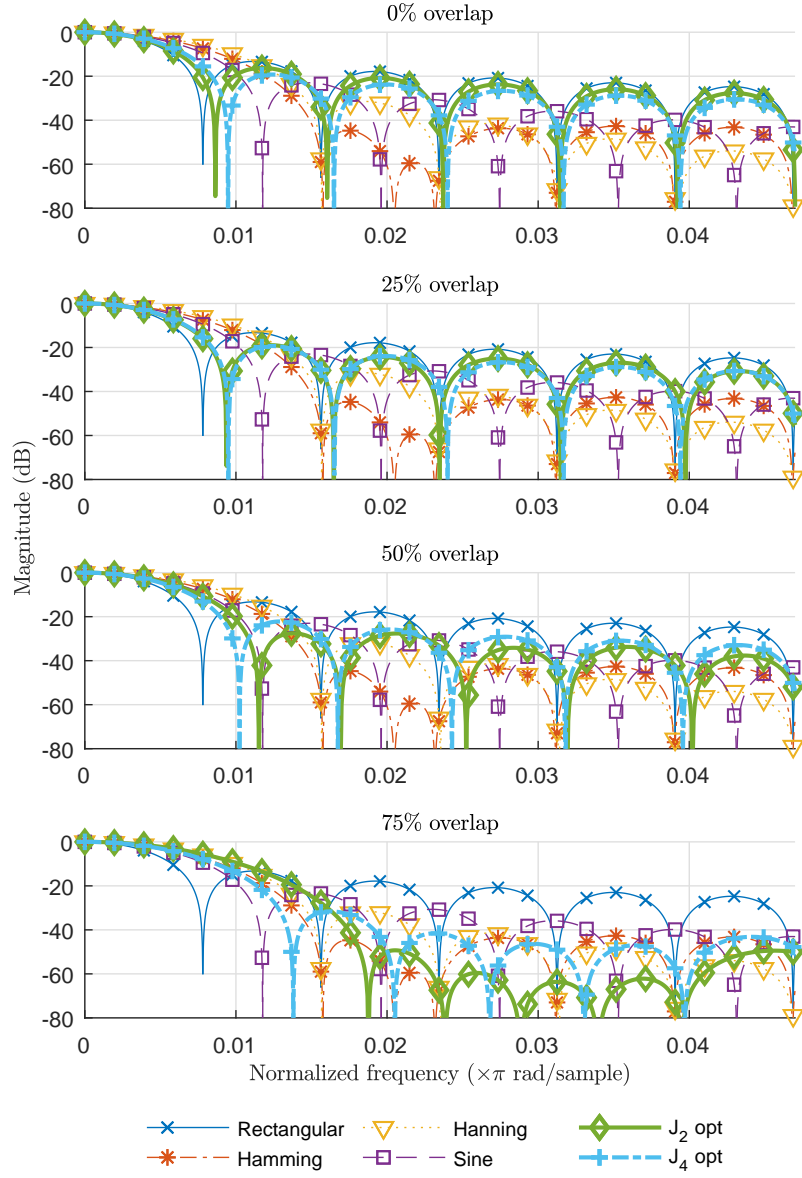
18

Figure 4: Comparison of the spectra of the proposed windows ($N = 256$) with other non-optimized windows, for different overlap factors.

may be of interest to apply pre-compensation directly during the OLA synthesis stage. Note that, given a "quasi-stationary" window with $r_w[n;\tau] \approx r_w[\tau]$, a naive pre-compensation scheme which obtains $r_x[\tau]$ as $r_x[\tau] = r_z[\tau]/r_w[\tau]$ (with $r_z[\tau]$ the desired autocorrelation values for the synthesized process) may run into trouble if $r_w[\tau]$ is close to zero; and even if this is not the case, the resulting $r_x[\tau]$ need not be a valid autocorrelation sequence, in the sense that its Fourier transform may not be non-negative at all frequencies. Thus, spectral pre-compensation is not a trivial problem and is left for future work.

Fig. 5 compares the results obtained in terms of the cost functions $J_2$ and $J_4$ for six different windows: rectangular, Hamming, Hanning, Sine, $J_2$- and $J_4$-optimized. The $J_2$- and $J_4$-based designs yield similar performance for overlap factors below 50%. Above this value, their differences become more pronounced, although both designs result in good behavior with respect to either cost. The optimized windows outperform other alternatives over the whole overlap range.

If a tradeoff between second- and fourth-order stationarity is desired, one may consider the minimization of a convex combination of costs, i.e., $J(\boldsymbol{w}) = \eta J_2(\boldsymbol{w}) + (1 - \eta)J_4(\boldsymbol{w})$, with $0 \leq \eta \leq 1$ a design parameter. Minimization of $J(\boldsymbol{w})$ can be achieved iteratively, following the procedure described in Sec. 3.3, but replacing the matrix $\boldsymbol{A}(\boldsymbol{w})$ by $\eta\boldsymbol{A}(\boldsymbol{w}) + (1 - \eta)\boldsymbol{K}(\boldsymbol{w})$.

Fig. 6 shows the time fluctuations of the variance and of the kurtosis-related function $\rho_w[n]$ for the same windows, and for three different overlap percentages: 50%, 62.5% and 75%. Clearly, with larger overlap, the variance and the kurtosis become more constant. This is at the price of a more reduced range of allowable kurtoses, since the mean value of $\rho_w[n]$ tends to decrease with more overlapping (due to the aforementioned "Gaussianization" effect).

The time fluctuations may become apparent in the time domain for low overlap factors, as shown in Fig. 7 for 25%. For each type of synthesis window we show a segment of 20 seconds and an overlay of all successive blocks of 256 samples length. All the signals are synthesized with a duration of 600 s and a sample rate of 256 Hz, and correspond to a white random process with average kurtosis $\bar{\beta}_z = 4.83$. The variation in amplitude is clearly noticeable in both the
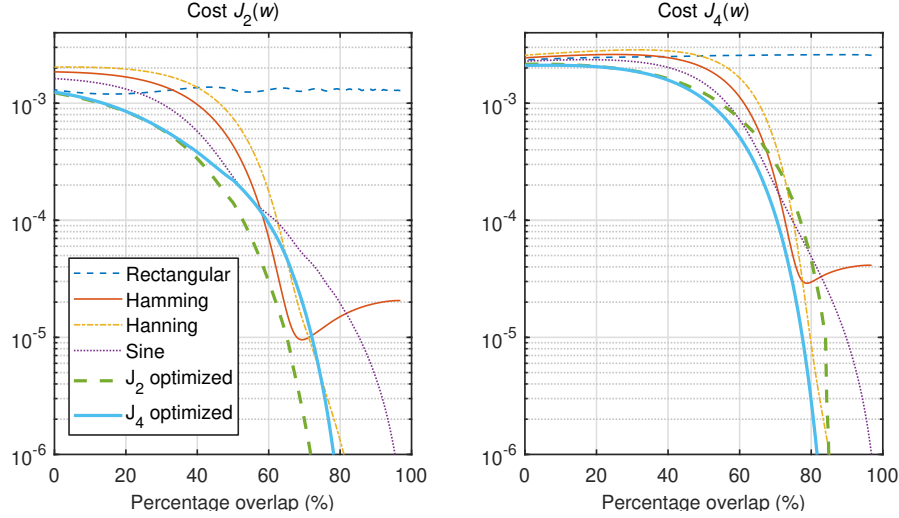
20

Figure 5: Results obtained for $N = 256$ and different overlap factors. Left: second-order cost $J_2(\boldsymbol{w})$. Right: fourth-order cost $J_4(\boldsymbol{w})$.

time signal and the block overlay, with the rectangular, $J_2$-optimized and $J_4$-optimized windows presenting the lowest observable amplitude variation. Fig. 8 presents the same white process synthesized with 50% overlap. In that case, the cyclic variation of the process variance and kurtosis is not as clearly identified in the time history, but becomes apparent in the block overlay for some of the synthesis windows, such has the Hamming and Hanning. This brings to light the fact that, although the process is indeed suffering from significant time fluctuations in both variance and kurtosis, a simple time domain inspection will not directly reveal it for most of the synthesis windows.

In a vibration control scenario, if the non-stationarity of the synthesized signal is not taken into account whereas the *average* kurtosis is adjusted by the control loop, the *peak* kurtosis will exceed the expected value, leading to an increase in the applied loads. For a better illustration of the variation of the actual kurtosis, the resulting values of $\beta_z[n]$ described by (37) with $\beta_x = 4.83$ are plotted in Fig. 9. The range of kurtosis variation and the trade-off between kurtosis range, stationarity and overlap level is clearly noticeable. A
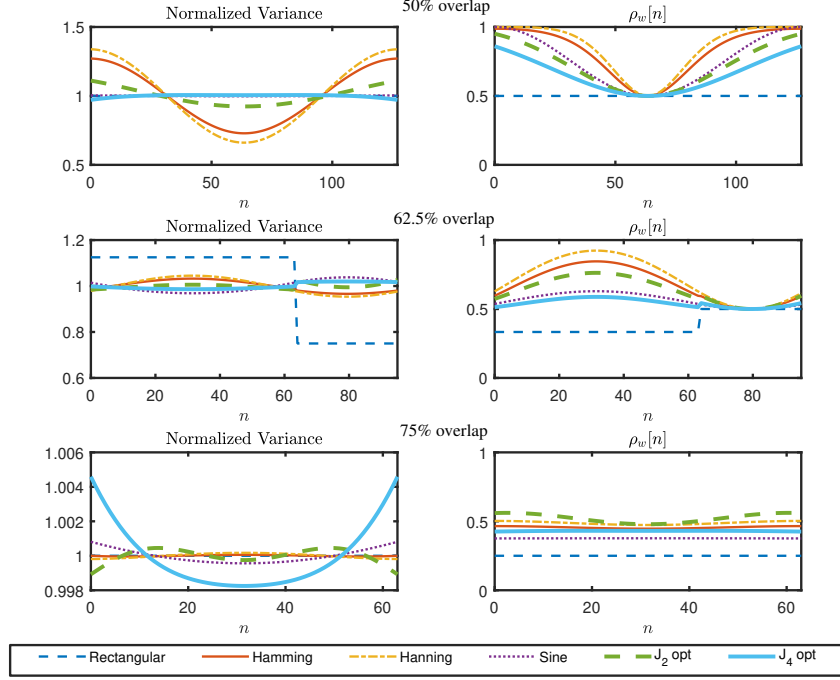
21

Figure 6: Time fluctuations over one period of the normalized variance and the kurtosis-related function $\rho_w[n]$ for $N = 256$ and three different overlap factors.

proper adjustment of the kurtosis level would then require compensation of the "Gaussianization" effect produced by the OLA processing. Directly increasing the kurtosis $\beta_x$ of the block process $x_\ell[n]$ without reducing the fourth-order non-stationarity would correct the average kurtosis, but it would also increase its range of variation, leading to an undesired increase in the peak load.

## 6. Conclusions

The proposed window design clearly improves the stationarity of random vibration signals synthesized by means of the overlap-add method, for both Gaussian and non-Gaussian cases, and provides a clear and simple criterion to quantify and optimize the stationarity of the synthesized process for any given overlap factor. The proposed iterative approach for the calculation of the
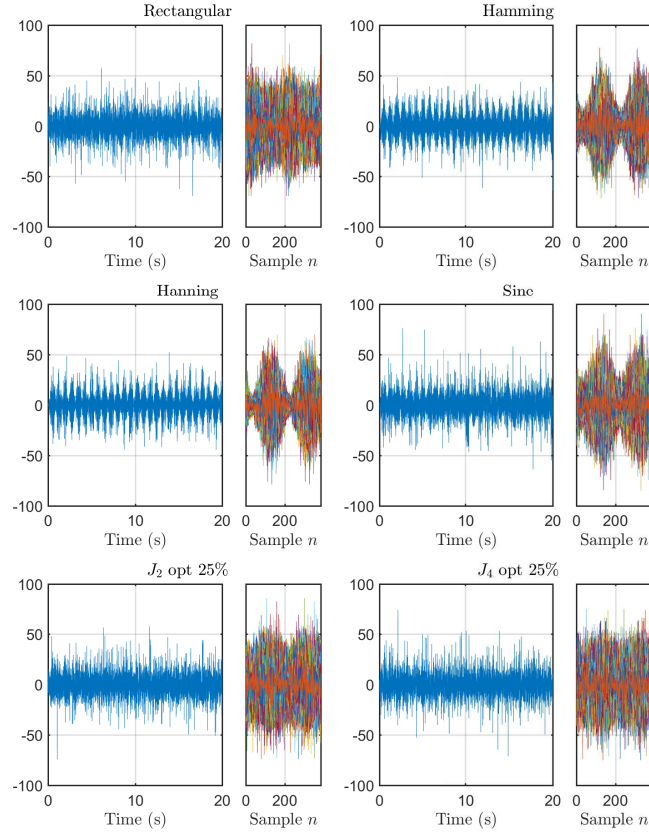
22

Figure 7: Time realization (left) and overlay of blocks of 256 samples length (right) of a white random process with kurtosis $\bar{\beta}_z = 4.83$ and $N = 256$, using different synthesis windows and 25% overlap.
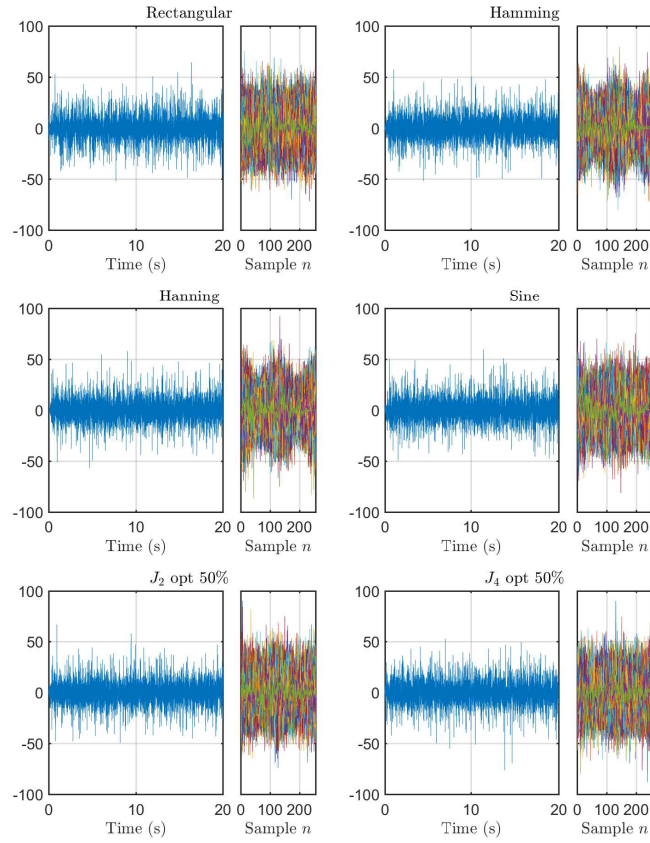
Figure 8: Time realization (left) and overlay of blocks of 256 samples length (right) of a white random process with average kurtosis $\bar{\beta}_z = 4.83$ and $N = 256$, using different synthesis windows and 50% overlap.
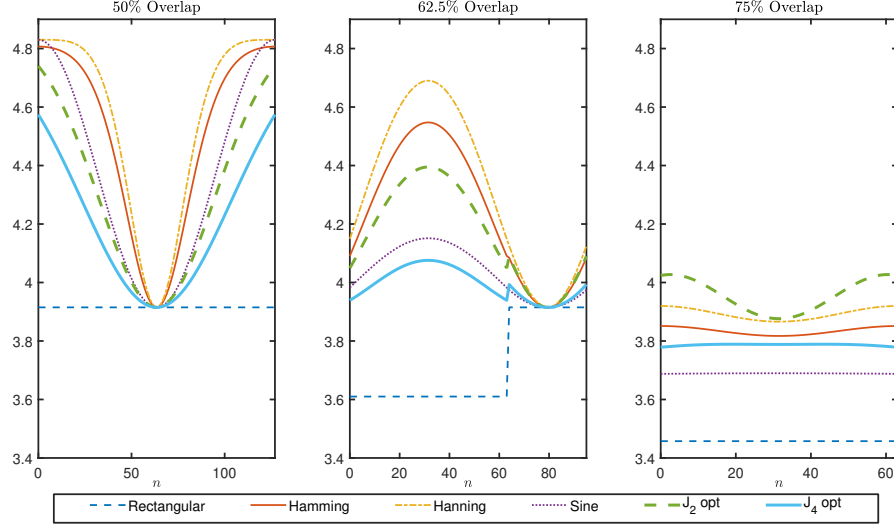
24

Figure 9: Time variations of the kurtosis for $\beta_x = 4.83$ and $N = 256$. Left: 50% overlap; middle: 62.5% overlap; right: 75% overlap.

optimal window is computationally simple; nevertheless, windows can be pre-computed and stored for their use in real-time applications. The stationarity analysis is particularly important for non-Gaussian synthesis, where an uncon-trolled cyclic variation of the process kurtosis may lead to significant increase of the crest factor and severity of the synthesized vibration. The proposed approach provides a criterion that minimizes undesired variability and hence allows better control of the fourth-order statistics of the synthesized random signal. Although in general larger overlap values lead to improved stationarity properties, this comes at the cost of an increase in computational load and a Gaussianization of the synthesized process, so that the choice of an adequate window allowing smaller overlap becomes all the more important.

25

## Appendix A. Proof of Lemma 1

Let $\overline{\boldsymbol{A}}_{\tau k} = \mathrm{Re}\{\boldsymbol{A}_{\tau k}\}$ and $\widetilde{\boldsymbol{A}}_{\tau k} = \mathrm{Im}\{\boldsymbol{A}_{\tau k}\}$. Then, since $\boldsymbol{w}$ is real-valued,

$$
\begin{aligned}
\nabla_{\boldsymbol{w}}\left|\boldsymbol{w}^T \boldsymbol{A}_{\tau k}\boldsymbol{w}\right|^2 &= \nabla_{\boldsymbol{w}}(\boldsymbol{w}^T\overline{\boldsymbol{A}}_{\tau k}\boldsymbol{w})^2 + \nabla_{\boldsymbol{w}}(\boldsymbol{w}^T\widetilde{\boldsymbol{A}}_{\tau k}\boldsymbol{w})^2 \\
&= 2(\boldsymbol{w}^T\overline{\boldsymbol{A}}_{\tau k}\boldsymbol{w}) \cdot \nabla_{\boldsymbol{w}}(\boldsymbol{w}^T\overline{\boldsymbol{A}}_{\tau k}\boldsymbol{w}) \\
&\quad + 2(\boldsymbol{w}^T\widetilde{\boldsymbol{A}}_{\tau k}\boldsymbol{w}) \cdot \nabla_{\boldsymbol{w}}(\boldsymbol{w}^T\widetilde{\boldsymbol{A}}_{\tau k}\boldsymbol{w}). \quad (\text{A.1})
\end{aligned}
$$

For any real-valued matrix $\boldsymbol{M}$ (not necessarily symmetric), it can be readily checked that $\nabla_{\boldsymbol{w}}(\boldsymbol{w}^T\boldsymbol{M}\boldsymbol{w}) = (\boldsymbol{M} + \boldsymbol{M}^T)\boldsymbol{w}$. Therefore, (A.1) reads as

$$
\begin{aligned}
\nabla_{\boldsymbol{w}}\left|\boldsymbol{w}^T \boldsymbol{A}_{\tau k}\boldsymbol{w}\right|^2 &= 2(\boldsymbol{w}^T\overline{\boldsymbol{A}}_{\tau k}\boldsymbol{w}) \cdot (\overline{\boldsymbol{A}}_{\tau k} + \overline{\boldsymbol{A}}_{\tau k}^T)\boldsymbol{w} \\
&\quad + 2(\boldsymbol{w}^T\widetilde{\boldsymbol{A}}_{\tau k}\boldsymbol{w}) \cdot (\widetilde{\boldsymbol{A}}_{\tau k} + \widetilde{\boldsymbol{A}}_{\tau k}^T)\boldsymbol{w} \quad (\text{A.2}) \\
&= 2\,\mathrm{Re}\left\{\boldsymbol{w}^T \boldsymbol{A}_{\tau k}^H\boldsymbol{w} \cdot (\boldsymbol{A}_{\tau k} + \boldsymbol{A}_{\tau k}^T)\boldsymbol{w}\right\} \quad (\text{A.3})
\end{aligned}
$$

Summing over $\tau$ and $k$,

$$
\begin{aligned}
\nabla_{\boldsymbol{w}} J_2(\boldsymbol{w}) &= 2\,\mathrm{Re}\left\{\frac{1}{D^2}\sum_{k=1}^{D-1}\sum_{|\tau|<N} \boldsymbol{w}^T \boldsymbol{A}_{\tau k}^H\boldsymbol{w} \cdot (\boldsymbol{A}_{\tau k} + \boldsymbol{A}_{\tau k}^T)\boldsymbol{w}\right\} \\
&= 2\,\mathrm{Re}\left\{\frac{1}{D^2}\sum_{k=1}^{D-1}\sum_{|\tau|<N} \boldsymbol{A}_{\tau k}\boldsymbol{w}\boldsymbol{w}^T\boldsymbol{A}_{\tau k}^H\boldsymbol{w}\right\} + 2\,\mathrm{Re}\left\{\frac{1}{D^2}\sum_{k=1}^{D-1}\sum_{|\tau|<N} \boldsymbol{A}_{\tau k}^T\boldsymbol{w}\boldsymbol{w}^T\boldsymbol{A}_{\tau k}^H\boldsymbol{w}\right\} \\
&= 2\,\mathrm{Re}\left\{\frac{1}{D^2}\sum_{k=1}^{D-1}\sum_{|\tau|<N} \boldsymbol{A}_{\tau k}\boldsymbol{w}\boldsymbol{w}^T\boldsymbol{A}_{\tau k}^H\boldsymbol{w}\right\} + 2\,\mathrm{Re}\left\{\frac{1}{D^2}\sum_{k=1}^{D-1}\sum_{|\tau|<N} \boldsymbol{A}_{\tau k}^T\boldsymbol{w}\boldsymbol{w}^T\boldsymbol{A}_{\tau k}^*\boldsymbol{w}\right\} \\
&= 2\,\mathrm{Re}\left\{\boldsymbol{A}(\boldsymbol{w}) + \boldsymbol{B}(\boldsymbol{w})\right\}\boldsymbol{w}, \quad (\text{A.4})
\end{aligned}
$$

where we have used (21)-(22) and the fact that $\boldsymbol{w}^T\boldsymbol{A}_{\tau k}^H\boldsymbol{w} = \boldsymbol{w}^T\boldsymbol{A}_{\tau k}^*\boldsymbol{w}$ because $\boldsymbol{w}$ is real-valued.

26

**Appendix B. Proof of Lemma 2**

Let us write the matrix $\boldsymbol{A}(\boldsymbol{w})$ as

$$
\begin{aligned}
\boldsymbol{A}(\boldsymbol{w}) &= \frac{1}{D^2} \sum_{k=1}^{D-1} \sum_{|\tau|<N} \boldsymbol{A}_{\tau k} \boldsymbol{w}\boldsymbol{w}^T \boldsymbol{A}_{\tau k}^H \\
&= \frac{1}{D^2} \sum_{k=1}^{D-1} \sum_{|\tau|<N} \boldsymbol{S}^\tau \boldsymbol{\Gamma}^k \boldsymbol{w}\boldsymbol{w}^T (\boldsymbol{\Gamma}^*)^k \left(\boldsymbol{S}^T\right)^\tau \qquad &\text{(B.1)} \\
&= \frac{1}{D^2} \sum_{|\tau|<N} \boldsymbol{S}^\tau \left(\sum_{k=1}^{D-1} (\boldsymbol{\Gamma}^k \boldsymbol{w})(\boldsymbol{\Gamma}^k \boldsymbol{w})^H\right) \left(\boldsymbol{S}^T\right)^\tau \qquad &\text{(B.2)} \\
&= \frac{1}{D^2} \sum_{|\tau|<N} \boldsymbol{S}^\tau \boldsymbol{Z}(\boldsymbol{w}) \left(\boldsymbol{S}^T\right)^\tau, \qquad &\text{(B.3)}
\end{aligned}
$$

where we have introduced

$$
\boldsymbol{Z}(\boldsymbol{w}) \triangleq \sum_{k=1}^{D-1} (\boldsymbol{\Gamma}^k \boldsymbol{w})(\boldsymbol{\Gamma}^k \boldsymbol{w})^H. \qquad \text{(B.4)}
$$

Due to the shift property of the matrices $\boldsymbol{S}$ and $\boldsymbol{S}^T$, it can be easily checked that $\boldsymbol{A}(\boldsymbol{w})$ is (Hermitian) Toeplitz, and therefore it is completely determined by the elements of its first column. These are given by

$$
[\boldsymbol{A}(\boldsymbol{w})]_{i,0} = \frac{1}{D^2} \sum_{\ell=0}^{N-1-i} [\boldsymbol{Z}(\boldsymbol{w})]_{i+\ell,\ell} \qquad i = 0, 1, \ldots, N-1, \qquad \text{(B.5)}
$$

or, in words, $[\boldsymbol{A}(\boldsymbol{w})]_{i,0}$ is obtained by summing the elements in the $i$-th subdiagonal of $\boldsymbol{Z}(\boldsymbol{w})$, and then dividing by $D^2$. Now, let us denote the $\ell$-th column of the $N \times N$ identity matrix (counting from $\ell = 0$ to $\ell = N-1$) by $\boldsymbol{e}_\ell$. Then

$$
\begin{aligned}
[\boldsymbol{Z}(\boldsymbol{w})]_{i+\ell,\ell} &= \boldsymbol{e}_{i+\ell}^H \boldsymbol{Z}(\boldsymbol{w}) \boldsymbol{e}_\ell \\
&= \sum_{k=1}^{D-1} (\boldsymbol{e}_{i+\ell}^H \boldsymbol{\Gamma}^k \boldsymbol{w})(\boldsymbol{e}_\ell^H \boldsymbol{\Gamma}^k \boldsymbol{w})^H \qquad &\text{(B.6)} \\
&= \sum_{k=1}^{D-1} (e^{-j\frac{2\pi}{D}k(i+\ell)} \boldsymbol{e}_{i+\ell}^H \boldsymbol{w})(e^{-j\frac{2\pi}{D}k\ell} \boldsymbol{e}_\ell^H \boldsymbol{w})^H \qquad &\text{(B.7)} \\
&= \alpha[i] w[i+\ell] w[\ell], \qquad &\text{(B.8)}
\end{aligned}
$$

where

$$
\alpha[i] \triangleq \sum_{k=1}^{D-1} e^{-j\frac{2\pi}{D}ki} = \begin{cases} D-1, & i = 0, \pm D, \pm 2D, \ldots, \\ -1, & \text{otherwise.} \end{cases} \qquad \text{(B.9)}
$$

27

Therefore, from (B.5) and (B.8), the elements of $\boldsymbol{A}(\boldsymbol{w})$ can be efficiently obtained from the autocorrelation of the window, as follows:

$$[\boldsymbol{A}(\boldsymbol{w})]_{i,0} = \frac{\alpha[i]}{D^2} \sum_{\ell=0}^{N-1-i} w[i+\ell]w[\ell] \qquad i = 0, 1, \ldots, N-1, \qquad \text{(B.10)}$$

which also shows that $\boldsymbol{A}(\boldsymbol{w})$ is real-valued. Regarding $\boldsymbol{B}(\boldsymbol{w})$, one has:

$$
\begin{aligned}
\boldsymbol{B}(\boldsymbol{w}) &= \frac{1}{D^2} \sum_{k=1}^{D-1} \sum_{|\tau|<N} \boldsymbol{A}_{\tau k}^T \boldsymbol{w}\boldsymbol{w}^T \boldsymbol{A}_{\tau k}^* \\
&= \frac{1}{D^2} \sum_{k=1}^{D-1} \sum_{|\tau|<N} \boldsymbol{\Gamma}^k \left(\boldsymbol{S}^T\right)^\tau \boldsymbol{w}\boldsymbol{w}^T \boldsymbol{S}^\tau (\boldsymbol{\Gamma}^*)^k && \text{(B.11)} \\
&= \frac{1}{D^2} \sum_{k=1}^{D-1} \boldsymbol{\Gamma}^k \left( \sum_{|\tau|<N} \left(\boldsymbol{S}^T\right)^\tau \boldsymbol{w}\boldsymbol{w}^T \boldsymbol{S}^\tau \right) (\boldsymbol{\Gamma}^*)^k && \text{(B.12)} \\
&= \frac{1}{D^2} \sum_{k=1}^{D-1} \boldsymbol{\Gamma}^k \boldsymbol{Y}(\boldsymbol{w})(\boldsymbol{\Gamma}^*)^k && \text{(B.13)}
\end{aligned}
$$

where we have introduced

$$\boldsymbol{Y}(\boldsymbol{w}) \triangleq \sum_{|\tau|<N} \left(\boldsymbol{S}^T\right)^\tau \boldsymbol{w}\boldsymbol{w}^T \boldsymbol{S}^\tau. \qquad \text{(B.14)}$$

Again, due to the shift property of $\boldsymbol{S}$ and $\boldsymbol{S}^T$, it can be easily checked that $\boldsymbol{Y}(\boldsymbol{w})$ is just the autocorrelation matrix of the window, i.e., it is symmetric Toeplitz with first column given by

$$[\boldsymbol{Y}(\boldsymbol{w})]_{i,0} = \sum_{\ell=0}^{N-1-i} w[i+\ell]w[\ell] \qquad i = 0, 1, \ldots, N-1. \qquad \text{(B.15)}$$

Therefore we can write the elements in the $i$-th subdiagonal of $\boldsymbol{B}(\boldsymbol{w})$ as

$$
\begin{aligned}
[\boldsymbol{B}(\boldsymbol{w})]_{i+p,p} &= \frac{1}{D^2} \boldsymbol{e}_{i+p}^H \boldsymbol{Y}(\boldsymbol{w})\boldsymbol{e}_p \\
&= \frac{1}{D^2} \sum_{k=1}^{D-1} \boldsymbol{e}_{i+p}^H \boldsymbol{\Gamma}^k \boldsymbol{Y}(\boldsymbol{w})(\boldsymbol{\Gamma}^*)^k \boldsymbol{e}_p && \text{(B.16)} \\
&= \frac{1}{D^2} \sum_{k=1}^{D-1} e^{-j\frac{2\pi}{D}k(i+p)} \boldsymbol{e}_{i+p}^H \boldsymbol{Y}(\boldsymbol{w})\boldsymbol{e}_p e^{j\frac{2\pi}{D}kp} && \text{(B.17)} \\
&= \frac{1}{D^2} \left(\boldsymbol{e}_{i+p}^H \boldsymbol{Y}(\boldsymbol{w})\boldsymbol{e}_p\right) \sum_{k=1}^{D-1} e^{-j\frac{2\pi}{D}ki} && \text{(B.18)} \\
&= \frac{\alpha[i]}{D^2} [\boldsymbol{Y}(\boldsymbol{w})]_{i+p,p}. && \text{(B.19)}
\end{aligned}
$$

Since $\boldsymbol{Y}(\boldsymbol{w})$ is Toeplitz, $[\boldsymbol{Y}(\boldsymbol{w})]_{i+p,p}$ depends only on $i$ but not on $p$. Thus, (B.19) shows that $\boldsymbol{B}(\boldsymbol{w})$ is Toeplitz as well, and using (B.15), its first column is given by

$$[\boldsymbol{B}(\boldsymbol{w})]_{i,0} = \frac{\alpha[i]}{D^2} \sum_{\ell=0}^{N-1-i} w[i+\ell]w[\ell]. \tag{B.20}$$

From (B.10) and (B.20), clearly $\boldsymbol{B}(\boldsymbol{w}) = \boldsymbol{A}(\boldsymbol{w})$, which concludes the proof.

### Acknowledgements

### References

[1] F. J. Harris, On the use of windows for harmonic analysis with the discrete Fourier transform, Proceedings of the IEEE 66 (1) (1978) 51–83.

[2] A. V. Oppenheim, R. W. Schafer, Discrete-time signal processing, Prentice-Hall, Upper Saddle River, NJ, USA, 1988.

[3] C. Borß, R. Martin, On the construction of window functions with constant-overlap-add constraint for arbitrary window shifts, in: Int. Conf. Acoustics, Speech and Signal Processing (ICASSP), IEEE, 2012, pp. 337–340.

[4] D. Smallwood, T. L. Paez, A frequency domain method for the generation of partially coherent normal stationary time domain signals, Shock and Vibration 1 (1) (1993) 45–53.

[5] D. O. Smallwood, Generation of partially coherent stationary time histories with non-Gaussian distributions, Tech. rep., Sandia National Labs., Albuquerque, NM (United States) (1996).

[6] A. Steinwolf, Random vibration testing with kurtosis control by IFFT phase manipulation, Mechanical Systems and Signal Processing 28 (2012) 561 – 573.

[7] P. Hanna, M. Desainte-Catherine, Adapting the overlap-add method to the synthesis of noise, in: Proceedings of the Digital Audio Effects Workshop (DAFX'02, Hamburg, Germany), 2002, pp. 101–104.

[8] D. Smallwood, Vibration with non-gaussian noise, Journal of the IEST 52 (2) (2009) 13–30.

[9] V. Rouillard, M. A. Sek, Synthesizing nonstationary, non-Gaussian random vibrations, Packaging Technology and Science 23 (2010) 423–439.

[10] F. Xu, C. Li, T. Jiang, On the shaker simulation of wind-induced non-Gaussian random vibration, Shock and Vibration 2016, article ID 5450865.

[11] F. Kihm, N. S. Ferguson, J. Antoni, Fatigue life from kurtosis controlled excitations, Procedia Engineering 133 (2015) 698 – 713, fatigue Design 2015, International Conference Proceedings, 6th Edition.

[12] J. Antoni, Cyclostationarity by examples, Mechanical Systems and Signal Processing 23 (4) (2009) 987 – 1036.

[13] G. B. Giannakis, Cyclostationary signal analysis, Digital Signal Processing Handbook (1998) 17–1.

[14] G. H. Golub, C. F. Van Loan, Matrix computations, Vol. 3, JHU Press, 2012, pp. 394–395.

[15] A. Brandt, Noise and Vibration Analysis: Signal Analysis and Experimental Procedures, Wiley, Chichester, West Sussex, UK, 2011.

[16] R. G. T. De Almeida, S. A. Da Silva Vicente, L. R. Padovese, New technique for evaluation of global vibration levels in rolling bearings, Shock and Vibration 9 (2002) 225–234.

[17] D. González, R. López-Valcarce, Spectral and statistical evaluation of the properties of the vibration measured at the base of an automotive seat for non-gaussian random noise synthesis, in: Proceedings of the International Conference on Noise and Vibration Engineering, in press 2018.

380